Inorganic Chemistry
Article

Inorg. Chem. **2009**, *48*, 6287–6296 **6287**
DOI: 10.1021/ic900575r

Can Electrospray Mass Spectrometry Quantitatively Probe Speciation? Hydrolysis of Uranyl Nitrate Studied by Gas-Phase Methods

Nikos G. Tsierkezos,[†,‡] Jana Roithová,[†,§] Detlef Schröder,[†,*] Milan Ončák,[∥,⊥] and Petr Slavíček[∥,⊥]

[†]*Institute of Organic Chemistry and Biochemistry, v.v.i., Academy of Sciences of the Czech Republic,* [‡]*Flemingovo nám. 2, 166 10 Prague 6, Czech Republic, Fachgebiet Chemie, Technische Universität Ilmenau, Weimarer Str. 25, 98693 Ilmenau, Germany,* [§]*Department of Organic and Nuclear Chemistry, Charles University in Prague, Hlavova 8, 12843 Prague 2, Czech Republic,* [∥]*Institute of Chemical Technology Prague, Technická 5, 16628 Prague 6, Czech Republic, and* [⊥]*J. Heyrovský Institute of Physical Chemistry, v.v.i., Academy of Sciences of the Czech Republic, Dolejškova 3, 18223 Prague 8, Czech Republic*

Received March 24, 2009

Electrospray ionization of uranyl nitrate dissolved in water generates gaseous species containing either hydroxo−uranyl $[UO_2(OH)]^+$ or nitrato−uranyl $[UO_2(NO_3)]^+$ contact ion pairs solvated by up to four water molecules. Furthermore, uranyl clusters of the general type $[U_mO_{2m}(X,Y)_{2m-1}(H_2O)_n]^+$ (X,Y = OH, NO_3) with m = 1−5 and n = 2−4 are formed. Collision-induced dissociation experiments are used to probe the structures and the stoichiometries of the uranyl ions generated. A detailed investigation of the concentration-dependent behavior of the formed gaseous uranyl complexes reveals a preference for nitrate- over hydroxide-containing species with increasing concentration of the sprayed solution. This behavior reflects changes in the pH value of the bulk solutions that can be attributed to solvolysis of UO_2^{2+} in water. Further, the tendency for generation of polynuclear cluster ions is amplified with increasing concentration and can be explained by a mechanism which involves the association of cations present in solution with neutral species such as $UO_2(OH)_2$, $UO_2(OH)(NO_3)$, and $UO_2(NO_3)_2$. The observed dependences of the cluster-ion intensities in the mass spectra from the concentration of the solutions fed to the electrospray source are used to suggest a scheme for a quantitative correlation between the gas-phase and solution-phase data. The results inter alia indicate that the effective concentrations of the spraying solution can be several orders of magnitude larger than those of the feed solutions entering the electrospray ionization source.

Introduction

In recent years, interest in the gas-phase chemistry of actinide (5f-block) ions, particularly uranium ions, increased significantly.[1−3] The speciation and the reactivity of uranium is a topic of continuous interest due to the relevance of species-dependent chemistry in nuclear-fuel processing and the mobility and fate of uranium in the geologic subsurface.[4] Given that uranium appears in higher oxidation states in the environment, principally +IV and +VI, considerable research interest is focused on the condensed and gas-phase chemistry of U(IV) and U(VI) ions. Thus, the coordination properties of the uranium ions commonly encountered in solution, namely, uranyl UO_2^{2+} and uranous U^{4+} ions, have been previously experimentally[5,6] and theoretically[7,8] investigated. For monodentate ligands, such as water or alcohols, the most common coordination number for UO_2^{2+} is five, while with the presence of bidentate ligands, such as oxalate or malonate, the coordination number increases to six. The water ligands can be easily replaced by NO_3^-, Cl^-, or Br^- ions.[9] In the solid state, coordination numbers of four, five, and six are common for monodentate ligands, while bidentate ligands can also support higher coordinations.[10] Uranium(IV) even tends to form nine- or higher coordinated

*To whom correspondence should be addressed. Phone: 00420 220 183 463. E-mail: Detlef.Schroeder@uochb.cas.cz.

(1) Jackson, G. P.; Gibson, J. K.; Duckworth, D. C. *Int. J. Mass Spectrom.* **2002**, *220*, 419.
(2) Gibson, J. K. *Int. J. Mass Spectrom.* **2002**, *214*, 1.
(3) Privalov, T.; Schimmelpfennig, B.; Wahlgren, U.; Grenthe, I. *J. Phys. Chem. A* **2002**, *106*, 11277.
(4) Brookins, D. G. *Geochemical Aspects of Radioactive Waste Disposal*; Springer-Verlag: New York, 1984.
(5) Dent, A. J.; Ramsay, J. D. F.; Swanton, S. W. *J. Colloid Interface Sci.* **1992**, *150*, 45.
(6) Nguyen-Trung, C.; Palmer, D. A.; Begun, G. M.; Peiffert, C.; Mesner, R. E. *J. Sol. Chem.* **2000**, *29*, 101.
(7) Spencer, S.; Gagliardi, L.; Handy, N. C.; Ioannou, A. G.; Skylaris C.-K.; Willetts, A.; Simper, A. M. *J. Phys. Chem. A* **1999**, *103*, 1831.
(8) (a) Clavaguere-Sarrio, C.; Brenner, V.; Hoyau, S.; Marsden, C. J.; Millie, P.; Dognon, J.-P. *J. Phys. Chem. B* **2003**, *107*, 3051. (b) Frick, R. J.; Pribil, A. B.; Hofer, T. S.; Randolf, B. R.; Bhattacharjee, A.; Rode, B. M. *Inorg. Chem.* In press, DOI: 10.1021/ic801554p.
(9) Berg, M.; Ferri, D.; Glaser, J.; Grenthe, I. *Inorg. Chem.* **1983**, *22*, 3986.
(10) Greenwood, N. N.; Earnshaw, A. *Chemistry of the Elements*, 2nd ed.; Butterworth Heinemann: Oxford, UK, 1997.

Published on Web 05/06/2009

complexes in the condensed phase as a result of its high charge.[11] Electrochemical studies indicate that UO_2^{2+} can be reversibly or quasi-reversibly reduced to UO_2^{+}, that is, uranium(V), in aqueous and nonaqueous media.[12] However, the solution chemistry of UO_2^{+} is difficult to study because U(V) rapidly undergoes disproportionation according to the formal process: $2UO_2^{+} \rightarrow UO_2 + UO_2^{2+}$.[13]

The bare uranyl dication UO_2^{2+} has been generated in the gas phase by reactions of U^{2+} with O_2 and N_2O.[14] According to these studies, the UO_2^{2+} dication seems to be thermodynamically stable toward Coulomb explosion to singly charged ions; note that despite the high charge even the diatomic species UF^{3+} is a thermochemically stable molecular trication.[15] Recently, several UO_2^{2+} species have been extensively studied using electrospray ionization mass spectrometry (ESI-MS),[16,17] which is a powerful tool for the generation of gaseous uranium ions in high oxidation states. For instance, Rasilis and Pemberton[18] applied ESI-MS for a detailed examination of uranyl(VI) citrate in aqueous solutions and observed pH-induced changes in the stoichiometry and coordination environment of the uranyl−citrate complexes formed. Furthermore, Van Stipdonk and co-workers extensively applied ion-trap mass spectrometry for the characterization of gaseous uranyl monocations and dications formed upon ESI of uranyl nitrate dissolved in water or in mixtures of water with acetone,[19] alcohols,[20,21] and nitriles.[22] From these studies, it has been concluded that the gas-phase behavior of UO_2^{2+} resembles the situation in solution. Recently, several mononuclear uranyl complexes were also characterized by infrared spectra of mass-selected ions in the gas phase.[23] However, despite these extensive investigations of UO_2^{2+} complexes, the molecular details of the solvation of uranyl salts in water and in particular the formation of polynuclear uranium(VI) clusters are not well-established so far. Infrared spectra of millimolar aqueous solutions of uranyl nitrate, $UO_2(NO_3)_2$, for example, indicate the presence of trinuclear as well as mononuclear species at low concentrations; the parallel existence of mono-, di-, and trinuclear complexes at medium concentrations; and the prevalence of dinuclear clusters at the highest concentrations studied.[24] Such an ordering of the oligomeric species prevailing in equilibrium appears quite unusual and would imply the existence of pronounced cooperative effects. Furthermore, these results are in conflict with potentiometric data which deny the occurrence of any kind of aggregation in pure aqueous uranyl−nitrate solutions up to concentrations of 0.14 mol L^{-1}.[25] It is thus obvious that a complementary method for the investigation of the molecular species formed upon ion speciation would be a conceptual step forward, provided a proof of principle can be delivered.

In the present study, ESI-MS is used for the generation and the characterization of gaseous uranyl complexes evolving from aqueous uranyl(VI)−nitrate solutions. The prevalent cationic species upon ESI are monocationic hydroxo−uranyl $[UO_2(OH)(H_2O)_n]^{+}$ as well as nitrato−uranyl $[UO_2(NO_3)(H_2O)_n]^{+}$ complexes coordinated by up to four water molecules. In addition, several polynuclear uranyl clusters, $[U_mO_{2m}(X,Y)_{2m-1}(H_2O)_n]^{+}$ with X and Y = OH and NO_3 and m = 2−5, are detected. In addition to the identification and characterization of these gaseous ions, a major purpose of the present work is to probe the usefulness of ESI-MS for the investigation of speciation behavior of uranyl nitrate in aqueous solution.[26] Similar studies may hence be used for the analysis of the speciation behavior of other high-valent actinides which are more difficult to study experimentally due to higher radioactivity.[27,28] The necessity for such complementary studies in element speciation using new approaches has been highlighted only recently in a detailed spectroscopic study of uranyl carbonate, which has questioned the seemingly well-established knowledge about the speciation of uranyl salts in its foundations.[29]

Methods

The experiments were performed with a TSQ Classic mass spectrometer, which has been described previously.[30] Briefly, the TSQ Classic consists of an ESI source combined with a tandem mass spectrometer of QOQ configuration (Q stands for quadrupole and O for octupole). The ions were generated by ESI of aqueous solutions of uranyl nitrate, which were infused into the ESI source using a syringe pump at a flow rate of 5 μL min^{-1}. The temperature of the heated capillary was maintained at 200 °C. In ESI, the size of the metal-ion solvates $ML_n^{\pm}$ generated very much depends on the source conditions, which can be varied from very soft (large n) to moderate (medium values of n) to hard (n = 0, 1);[31,32] reasonably soft conditions were applied in this work. The

(11) In comparing the coordination numbers of U^{4+} and UO_2^{2+}, it has to be noted that the former species is atomic whereas the latter is a molecule; thus, the uranium in UO_2^{2+} already bears two coordination atoms. In the following, we hence refer to the atomistic viewpoint.

(12) Mizuoka, K.; Kim, S.-Y.; Hasegawa, M.; Hoshi, T.; Uchiyama, G.; Ikeda, Y. *Inorg. Chem.* **2003**, *42*, 1031.
(13) See also: Belal, N.; Frisch, M., Ilton, E. S.; Ravel, B.; Cahill, C. L. *Inorg. Chem.* **2008**, *47*, 10135.
(14) Cornehl, H. H.; Heinemann, C.; Marcalo, J.; Pires de Matos, A.; Schwarz, H. *Angew. Chem., Int. Ed. Engl.* **1996**, *35*, 891.
(15) Schröder, D.; Diefenbach, M.; Klapötke, T. M.; Schwarz, H. *Angew. Chem., Int. Ed. Engl.* **1999**, *38*, 137.
(16) (a) Yamashita, M.; Fenn, J. B. *J. Phys. Chem.* **1984**, *88*, 4451. (b) Fenn, J. B. *J. Am. Soc. Mass Spectrom.* **1993**, *4*, 524.
(17) Jayaweera, P.; Blades, A. T.; Ikonomou, M. G.; Kebarle, P. *J. Am. Chem. Soc.* **1990**, *112*, 2452.
(18) Pasilis, S. P.; Pemberton, J. E. *Inorg. Chem.* **2003**, *42*, 6793.
(19) Van Stipdonk, M. J.; Chien, W.; Anbalagan, V.; Bulleigh, K.; Hanna, D.; Groenewold, G. S. *J. Phys. Chem. A* **2004**, *108*, 10448.
(20) Van Stipdonk, M. J.; Anbalagan, V.; Chien, W.; Gresham, G. L.; Groenewold, G. S.; Hanna, D. *J. Am. Soc. Mass Spectrom.* **2003**, *14*, 1205.
(21) Van Stipdonk, M. J.; Chien, W.; Anbalagan, V.; Gresham, G. L.; Groenewold, G. S. *Int. J. Mass Spectrom.* **2004**, *237*, 175.
(22) Van Stipdonk, M. J.; Chien, W.; Bulleigh, K.; Wu, Q.; Groenewold, G. S. *J. Phys. Chem. A* **2006**, *110*, 959.
(23) Groenewold, G. S.; Gianotto, A. K.; McIlwain, M. E.; Van Stipdonk, M. J.; Kullman, M.; Moore, D. T.; Polfer, N.; Oomens, J.; Infante, I.; Visscher, L.; Siboulet, B.; de Jong, W. A. *J. Phys. Chem. A* **2008**, *112*, 508.
(24) Tsushima, S.; Rossberg, A.; Ikeda, A.; Müller, K.; Scheinost, A. C. *Inorg. Chem.* **2007**, *46*, 10819.
(25) Azenha, M. E. D. G.; Burrows, H. D.; Formosinho, S. J.; Leitão, M. L. P.; Miguel, M. d.; Graca, M. *J. Chem. Soc., Dalton Trans.* **1998**, 2893.
(26) For a related quantitative study of the speciation of aluminium salts in water using ESI-MS, see: Urabe, T.; Tsugoshi, T.; Tanaka, M. *J. Mass. Spectrom.* **2009**, *44*, 193.
(27) For example, see: (a) Walther, C.; Fuss, M.; Büchner, S. *Radiochim. Acta* **2008**, *96*, 411. (b) Ayala, R.; Martinez, J. M.; Pappalardo, R. R.; Muñoz-Paez, A.; Marcos, E. S. *J. Phys. Chem. A* **2008**, *112*, 5416.
(28) (a) Moulin, C.; Charron, N.; Plancque, G.; Virelizier, H. *Appl. Spectrosc.* **2000**, *54*, 843. (b) Moulin, C.; Amekraz, B.; Hubert, S.; Moulin, V. *Anal. Chim. Acta* **2001**, *441*, 269.
(29) Müller, K.; Brendler, V.; Foersendorf, H. *Inorg. Chem. A* **2008**, *47*, 10127.
(30) (a) Roithová, J.; Schröder, D. *Phys. Chem. Chem. Phys.* **2007**, *9*, 713. (b) Roithová, J.; Schröder, D.; Mišek, J.; Stará, I. G.; Starý, I. *J. Mass Spectrom.* **2007**, *42*, 1233.
(31) Cech, N. B.; Enke, C. G. *Mass Spectrom. Rev.* **2001**, *20*, 362.
(32) Schröder, D.; Weiske, T.; Schwarz, H. *Int. J. Mass Spectrom.* **2002**, *219*, 729.

first quadrupole was used as a mass filter to scan mass spectra of the ions produced or to select the ions of interest. For CID, the mass-selected ions were guided through the octupole serving as a collision chamber followed by mass analysis of the ionic reaction products by means of the second quadrupole and subsequent detection. Xenon was used as a collision gas at pressures between 0.5×10^{-4} and 3×10^{-4} mbar, where the former corresponds to approximate single-collision conditions,[32] whereas larger pressures were applied to deliberately induce secondary fragmentations.

For the concentration series, a stock solution (2.0×10^{-2} mol L^{-1}) was prepared by dissolving the appropriate amount of uranyl nitrate hexahydrate, $UO_2(NO_3)_2 \cdot 6H_2O$, in deionized water and diluted to the desired concentrations ranging from 1.0×10^{-8} to 1.5×10^{-2} mol L^{-1}.

The calculations were performed using the density functional method B3LYP.[33] For uranium, the effective core potentials Stuttgart RLC in conjunction with CRENBL basis sets were used,[34] while the other atoms were described by the aug-cc-pVDZ basis sets as implemented in the Gaussian 03 suite.[35] As the results for mononuclear species with the CRENBL basis set on uranium have been found to be in excellent agreement with those for Stuttgart RLC (e.g., energies of formation are only slightly underestimated with average difference of 0.06 eV for 28 mononuclear species in the test set), the dinuclear species have been calculated employing the CRENBL basis. For all optimized structures, frequency analyses at the same level of theory were used in order to assign them as genuine minima or transition structures on the potential-energy surface (PES) as well as to calculate zero-point vibrational energies (ZPVEs). The relative energies (E_{rel}) of the structures given below thus refer to energies at 0 K. Further details are given in the Supporting Information.

Results and Discussion

Electrospray ionization of aqueous uranyl nitrate gives rise to various monocations of the general formula $[U_mO_{2m}(X,Y)_{2m-1}(H_2O)_n]^+$ with X and Y = OH and NO_3, of which the mononuclear species $[UO_2(X)(H_2O)_n]^+$ prevail in the entire range of concentrations studied (1.0×10^{-8} to 1.5×10^{-2} mol L^{-1}).[36] Despite careful searching, no gaseous uranyl dications could be observed under these conditions, which is in accordance with the previous ESI studies of Van Stipdonk and co-workers, who found gaseous dications only with dative ligands better than water[20,22] and also noted that only singly charged species are observed in the ESI spectra at capillary temperatures above 200 °C.[19] For six representative concentrations, the net formula, the mass-to-charge ratios (m/z), and the relative intensities of the solvated uranyl ions observed in the positive-ion ESI mass spectra are summarized in Table S1 (Supporting Information). With the exception of a few multiply solvated ions of low abundance, the assigned ion compositions were confirmed by CID experiments, of which a few representative examples are discussed below. The major aim of this work is to elucidate, whether there exist any direct correlations between the ESI mass spectra and the speciation of uranyl nitrate in aqueous solutions.[37,38] To this end, experiments at different concentrations were performed in order to assess and analyze the influence of the composition of the sprayed solution on the stoichiometries and the abundances of the gaseous uranyl complexes detected by mass spectrometry.

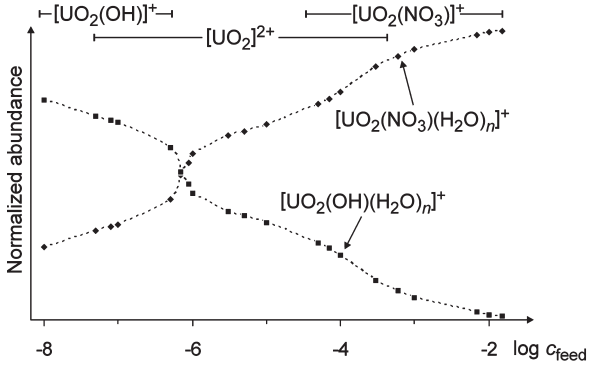

Figure 1. Normalized ion abundances of the mononuclear species $[UO_2(OH)(H_2O)_n]^+$ (■) and $[UO_2(NO_3)(H_2O)_n]^+$ (♦) as a function of the concentration of the sprayed solution (c_{feed}) in electrospray mass spectra of $UO_2(NO_3)_2$ in water. For both hydroxo- and nitrato complexes, the ions with $n = 3$ predominate under soft ionization conditions; the diagram shows the sum of all hydrated clusters, however. The horizontal bars qualitatively indicate the species existing in solution for the values of c_{spray} derived further below.[39,40]

The mononuclear uranyl complexes observed belong to the series $[UO_2(OH)(H_2O)_n]^+$ with $n = 1-4$ and $[UO_2(NO_3)(H_2O)_n]^+$ with $n = 0-4$. Under mild ionization conditions, the dominant species observed in the ESI mass spectra are the tris-hydrated monocations, $[UO_2(OH)(H_2O)_3]^+$ at m/z 341 and $[UO_2(NO_3)(H_2O)_3]^+$ at m/z 386, respectively. The number of water ligands n is independent of the concentration of the solution, as expected from the large excess of water used as a solvent. Further, the average coordination numbers (n_{av})[41,42] of $[UO_2(X)(H_2O)_n]^+$ agree within experimental error for the entire concentration range and for both counterions, that is, $n_{av} = 3.07 \pm 0.04$ for X = OH and $n_{av} = 3.04 \pm 0.07$ for X = NO_3. In marked contrast to the constant pattern of ion hydration, the relative abundances of hydroxo- versus nitrato complexes show a distinct dependence on the concentration of uranyl nitrate in solution (Figure 1). Thus, at concentrations below 5×10^{-7} mol L^{-1}, the hydroxo complex $[UO_2(OH)(H_2O)_3]^+$ dominates the ESI spectra. At increased concentrations, $[UO_2(OH)(H_2O)_3]^+$ and $[UO_2(NO_3)(H_2O)_3]^+$ have similar abundances, whereas above 1.0×10^{-6} mol L^{-1}, the nitrato complex

(33) (a) Becke, A. D. *J. Chem. Phys.* **1993**, *98*, 5648. (b) Vosko, S. H.; Wilk, L.; Nusair, M. *Can. J. Phys.* **1980**, *58*, 1200. (c) Lee, C.; Yang, W.; Parr, R. G. *Phys. Rev. B* **1988**, *37*, 785. (d) Miehlich, B.; Savin, A.; Stoll, H.; Preuss, H. *Chem. Phys. Lett.* **1989**, *157*, 200.

(34) (a) Küchle, W.; Dolg, M.; Stoll, H.; Preuss, H. *Mol. Phys.* **1991**, *74*, 1245. (b) Ermler, W. C.; Ross, R. B.; Christiansen, P. A. *Int. J. Quantum Chem.* **1991**, *40*, 829.

(35) *Gaussian 03*, revision C.02; Gaussian, Inc.: Wallingford CT, 2004.

(36) For high-resolution mass measurements, also see: Pasilis, S.; Somogyi, Á.; Herrmann, K.; Pembertoni, J. E. *J. Am. Soc. Mass Spectrom.* **2006**, *17*, 230.

(37) Di Marco, V. B.; Bombi, G. G. *Mass Spectrom. Rev.* **2006**, *25*, 347.

(38) Luedtke, W. D.; Landman, U.; Chiu, Y.-H.; Levandler, D. J.; Dressler, R. A.; Sok, S.; Gordon, M. S. *J. Phys. Chem. A* **2008**, *112*, 9628.

(39) Thermodynamic data taken from: Grenthe, I.; Fuger, J.; Konings, J. M.; Lemire, R. J.; Muller, A. B.; Nguyen Trung, C.; Wanner, H. *Chemical Thermodynamics of Uranium*; NEA-TDB, OECD Nuclear Energy Agency Data Bank: North Holland, Amsterdam, 1992.

(40) Given the recently articulated serious doubt about the speciation of uranium(VI) in water, specifically the large prevalence of free $(UO_2^{2+})_{aq}$ over a large concentration range ref 29, here we refrain from a detailed quantitative discussion of the condensed-phase data.

(41) The average coordination number of a hydrated cation $M(H_2O)_n^+$ is calculated as $n_{av} = \sum(n_i \times I(n)_i)/\sum I(n)_i$, where $I(n)$ stands for the abundance of a hydrated ion with n water ligands.

(42) (a) Tsierkezos, N. G.; Roithová, J.; Schröder, D.; Molinou, I. E.; Schwarz, H. *J. Phys. Chem. B* **2008**, *112*, 4365. (b) Schröder, D.; De Jong, K. P.; Roithová, *J. Eur. J. Inorg. Chem.* In press, DOI: 10.1002/ejic.200900050.

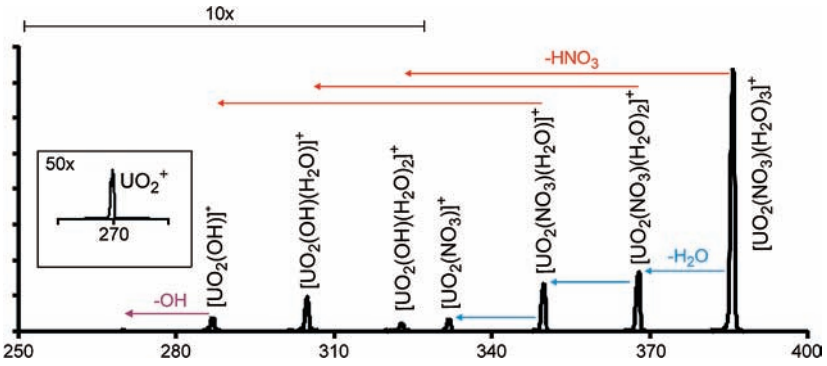

Figure 2. CID spectrum of mass-selected $[UO_2(NO_3)(H_2O)_3]^+$ (m/z 386) at a collision energy of E_{lab} = 20 eV at a xenon pressure of 2×10^{-4} mbar to deliberately include consecutive fragmentation in multiple collision events.

$[UO_2(NO_3)(H_2O)_3]^+$ prevails largely. Another, less pronounced change in slope occurs at about 10^{-4} mol L^{-1}. By reference to the concept of element speciation, we may tentatively assign these three regimes to solvated $UO_2(OH)^+$, UO_2^{2+}, and $UO_2(NO_3)^+$ as the cationic species being present in solution at the various concentrations.[39,40] Conceptually, it is important to point out that the concentration dependence demonstrates beyond any doubt that the ESI spectra qualitatively respond to the situation in the bulk solution;[43] possible quantitative relationships are addressed further below.[44]

$$UO_2^{2+} + H_2O \rightarrow [UO_2(OH)]^+ + H_{aq}^+ \qquad (1)$$

The switch from hydroxo- to nitrato complexes can be attributed to the decrease of the solution pH upon an increase of the uranyl−nitrate concentration.[39,45,46] It is well-known that the uranyl ion acts as a Lewis acid and participates in hydrolysis reactions, such a proton release according to reaction 1,[47,48] which lead finally to the formation of clusters such as $[U_2O_4(OH)_2]^{2+}$, $[U_2O_4(OH)_3]^+$, and $[U_2O_4(OH)_4]$.[49] Moulin et al.[50] have investigated the dependence of the complexation of the uranyl ion sampled via ESI in the gas phase from the solution pH. With the progressive increase of the pH of the solution, they observed replacement of the perchlorato ligand in $[UO_2(ClO_4)(H_2O)_n]^+$ by hydroxide to afford $[UO_2(OH)(H_2O)_n]^+$. Further, the dominance of $[UO_2(OH)(H_2O)_3]^+$ in the ESI spectra is in accordance with previous reports, in which it was experimentally confirmed that the dissociation rate of the trishydrated uranyl hydroxide is negligible, compared to other hydrated $[UO_2(OH)(H_2O)_n]^+$ species, and that 6 is a good coordination number for U(VI);[51] similar arguments can be put forward for the preferred observation of the nitrato complex $[UO_2(NO_3)(H_2O)_3]^+$ with three water ligands, but NO_3^- can also act as a bidentate ligand (see below).[52]

Collision-induced dissociation (CID) experiments were performed to elucidate the fragmentation pathways of the hydrated uranyl(VI) monocations. The major objective of the CID experiments is, however, to probe if all ions considered here can be regarded as "mere" solvates, or if specific redox reactions or bond-activation processes take place.[53,54] As a representative example, a CID spectrum of the coordinated complex $[UO_2(NO_3)(H_2O)_3]^+$ (m/z 386) is shown in Figure 2. At low collision energies (not shown), sequential eliminations of the three coordinating water molecules predominate. At elevated collision energy (E_{lab} = 20 eV), peaks at m/z 323, m/z 305, and m/z 287 are also observed which correspond to the hydroxo complexes $[UO_2(OH)(H_2O)_2]^+$, $[UO_2(OH)(H_2O)]^+$, and $[UO_2(OH)]^+$, respectively, concomitant with the elimination of neutral HNO_3. The loss of HNO_3 implies that a proton is transferred from a coordinating water molecule to the NO_3^- anion after the activating collision. Similar proton-transfer processes have been already observed upon CID of other gaseous metal−ion complexes,[28,54,55] and the occurrence in the case of the uranium complexes under

(43) See also: Sarpola, A. T.; Saukkoriipi, J. J.; Hietapelto, V. K.; Jalonen, J. E.; Jokela, J. T.; Joensuu, P. H.; Laasonen, K. E., Ramo, J. H. *Phys. Chem. Chem. Phys.* **2007**, *9*, 377.

(44) A reviewer argued that the ion distribution may entirely be due to the ESI process itself and hence independent of the situation in solution. While we cannot exclude the option that two independent processes, that is, heterolysis in solution and dynamic events in ESI, accidentally lead to similar results, the trends in Figure 1 correlate well with the change of pH in $UO_2(NO_3)_2$ solutions of different concentrations. The above distinction between processes in solution and in ESI thus becomes semantic, as one may also ask if the dynamical processes in ESI lead to ion distributions which correlate with the situation in solution.

(45) While one is tempted to use the data in Figure 1 to derive the solution pH, such a calculation is not possible because ESI only provides the ratio of the hydroxo- and nitrato-uranyl cations but does not give any information about the absolute fraction of heterolysis and thus the amount of intact, neutral uranyl nitrate present in solution. For pH values of $UO_2(NO_3)_2$ solutions in water, see ref 46.

(46) Botts, J. L.; Raridon, R. J.; Costanzo, D. A. *Density, Acidity and Conductivity Measurements of Uranyl Nitrate/Nitric Acid Solutions*; Oak Ridge National Laboratory, ORNL/TM-6491: Oak Ridge, TN, 1978.

(47) Antonchenko, V. Y.; Kryachko, E. S. *Theor. Chem. Acc.* **2008**, *120*, 421.

(48) Milic, N. B.; Suramji, T. M. *Z. Anorg. Allg. Chem.* **2004**, *489*, 197.

(49) Mashirov, L. G.; Mikhalev, V. A.; Suglobov, D. N. *Compt. Rend.* **2004**, *7*, 1179.

(50) Moulin, C.; Charron, N.; Plancque, G.; Virelizier, H. *Appl. Spectrosc.* **2000**, *54*, 843.

(51) Gresham, G. L.; Gianotto, A. K.; de, B.; Harrington, P. D.; Cao, L. B.; Scott, J. R.; Olson, J. E.; Appelhans, A. D.; Van Stipdonk, M. J.; Groenewold, G. S. *J. Phys. Chem. A* **2003**, *107*, 8530.

(52) See also: Jagoda-Cwiklik, B.; Jungwirth, P.; Rulíšek, L.; Milko, P.; Roithová, J.; Lemaire, J.; Maitre, P.; Ortega, J. M.; Schröder, D. *ChemPhysChem* **2007**, *8*, 1629.

(53) For redox reactions of gaseous metal-nitrate ions, see: (a) Cheng, Z. L.; Siu, K. M. W.; Guevremont, R.; Berman, S. S. *Org. Mass Spectrom.* **1992**, *27*, 1370. (b) Schröder, D.; Holthausen, M. C.; Schwarz, H. *J. Phys. Chem. B* **2004**, *108*, 14407. (c) Frański, R. *Eur. J. Mass Spectrom.* **2006**, *12*, 199. (d) Schröder, D.; Roithová, J. *Angew. Chem., Int. Ed.* **2006**, *45*, 5705. (e) Schröder, D.; Roithová, J.; Schwarz, H. *Int. J. Mass Spectrom.* **2006**, *254*, 197. (f) Roithová, J.; Schröder, D. *J. Am. Chem. Soc.* **2007**, *129*, 15311.

(54) For proton-transfer processes in microsolvated contact-ion pairs, see: (a) Akibo-Betts, G.; Barran, P. E.; Puskar, L.; Duncombe, B.; Cox, H.; Stace, A. J. *J. Am. Chem. Soc.* **2002**, *124*, 9257. (b) Trage, C.; Diefenbach, M.; Schröder, D.; Schwarz, H. *Chem.—Eur. J.* **2006**, *12*, 2454.

(55) Grüne, P.; Trage, C.; Schröder, D.; Schwarz, H. *Eur. J. Inorg. Chem.* **2006**, 4546.

Table 1. Binding Energies (in eV) of the Water Ligands in $[UO_2(OH)(H_2O)_n]^+$ and $[UO_2(NO_3)(H_2O)_n]^+$ Complexes and the Angle of the Uranyl Subunits (α_{OUO} in degrees) Calculated at the B3LYP/pVDZ Level of Theory

	n				
	0	1	2	3	4
$D(H_2O-UO_2(OH)(H_2O)_{n-1}^+)$		1.38	1.19	0.93	0.47
α_{OUO}	167°	168°	169°	170°	170°
$D(H_2O-UO_2(NO_3)(H_2O)_{n-1}^+)$		1.44	1.28	0.94	0.38
α_{OUO}	171°	172°	173°	174°	178°[a]

[a] This value refers to the lowest-lying structure having an η^2-nitrato ligand; an energetically close structure with η^1 coordination of the nitrato ligand and an additional hydrogen bond has $\alpha_{OUO} = 173°$.

study reiterates the solvolysis suggested to take place in the condensed phase.[56] Finally, a weak signal at *m*/*z* 270 is also observed at elevated collision energies, which corresponds to the UO_2^+ monocation and hence a reduction from U(VI) to U(V) concomitant with the loss of a neutral radical (i.e., $OH^•$ or $NO_3^•$).[57] We note, however, that this redox process is only observed at high collision energies and otherwise all uranium-containing ions formed upon can be assigned to the U(VI) valence state of the precursor compound.[58]

The fragmentation processes upon CID of mass-selected $[UO_2(OH)(H_2O)_3]^+$ (*m*/*z* 341, not shown) are perfectly analogous in that gradual elimination of water ligands leads to the formation of $[UO_2(OH)]^+$ (*m*/*z* 287), which finally loses an $OH^•$ radical at elevated collision energies to yield UO_2^+ (*m*/*z* 270) as the quasi-terminal fragment.

In order to achieve some information about the energetics of the hydrated species, ab initio calculations of $[UO_2(X)(H_2O)_n]^+$ with $n = 0-4$ and X = OH or NO_3 were performed, whose key results are summarized in Table 1. As expected for hydrated metal ions,[59] the water-binding energies decrease from about 1.4 eV for the first water ligand to slightly lower values (ca. 1.25 eV) for the second water ligand, even lower, but still reasonable, binding energies for the third water molecule (ca. 0.9 eV), and values below 0.5 eV for the fourth water ligand. The marked drop in binding energies between $n = 3$ and 4 can be attributed to the favorable quasi-octahedral coordination geometry of uranium in $[UO_2(X)(H_2O)_3]^+$ with two oxo ligands, one covalently bound counterion X, and three coordinating water molecules, such that a fourth water ligand must either distort the geometry to a higher coordination number of 7 or 8 (X = OH, NO_3) or be complexed in the second solvation sphere (X = NO_3). The slightly higher average bonding energies of the water molecules to the nitrato than to the hydroxo complexes can be assigned to geometric reasons, for example, to the values of α_{OUO} (Table 1). Thus, inspection of the computed geometries indicates a larger distortion of the

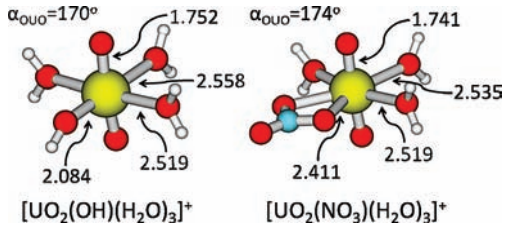

Figure 3. Computed structures of the energetically most stable confirmations of $[UO_2(OH)(H_2O)_3]^+$ and $[UO_2(NO_3)(H_2O)_3]^+$ with selected bond lengths (in Å) and the angle α_{OUO} (in degrees). For further details, see the Supporting Information.

geometry of the uranyl subunit in $[UO_2(OH)(H_2O)_3]^+$ in comparison to that of $[UO_2(NO_3)(H_2O)_3]^+$. This is reflected by the change of α_{OUO} of the uranyl subunit, such that the water ligand opposite the OH group in $[UO_2(OH)(H_2O)_3]^+$ bears a significantly longer U−O distance (2.558 Å) than those of the two other water molecules (2.519 Å), whereas these bond lengths are more balanced in the nitrato complex $[UO_2(NO_3)(H_2O)_3]^+$ (2.535 and 2.519 Å, respectively, Figure 3).[60]

Instructive with respect to the hydrolysis of uranyl nitrate to hydroxo complexes is the consideration of the energetics of the isodesmic reaction 2. For $n = 0$, that is, the nonsolvated neutral compounds, as well as throughout $n = 1-3$ (the hydrated neutral compounds), reaction 2 is computed to be endothermic by 0.32, 0.35, 0.12, and 0.21 eV, respectively, which is consistent with the experimentally found predominance of the hydroxo complexes at large dilution (Figure 1).

$$[UO_2(OH)(H_2O)_3]^+ + [UO_2(NO_3)_2(H_2O)_n] \rightarrow [UO_2(NO_3)(H_2O)_3]^+ + [UO_2(OH)(NO_3)(H_2O)_n] \quad (2)$$

Conceptually, the preference for the formation of the cationic hydroxo complexes can be explained by the distribution of the positive charge also to the hydrogen atom of the hydroxy group, whereas the nitrato ligand cannot serve for this purpose and only acts as an electronegative group.[61] At higher concentrations, the protons released upon uptake of hydroxide anions from solution act against a further buildup of proportional amounts of $[UO_2(OH)(H_2O)_n]^+$ (reaction 3), whereas heterolysis to neutral uranyl nitrate to afford $[UO_2(NO_3)_2(H_2O)_n]$ (reaction 4) is not affected by a decrease in pH.[62]

$$[UO_2(NO_3)(H_2O)_n]^+ + H_2O \rightarrow [UO_2(OH)(H_2O)_n]^+ + NO_3^- + H_{aq}^+ \quad (3)$$

$$[UO_2(NO_3)_2(H_2O)_n] \rightarrow [UO_2(NO_3)(H_2O)_n]^+ + NO_3^- \quad (4)$$

(56) See also: Garrison, S. L.; Becnel, J. M. *J. Phys. Chem. A* **2008**, *112*, 5453.

(57) For the occurrence reduction from U(VI) to U(V) under hydrothermal conditions, see ref 13.

(58) In fact, the valence state of the precursor compounds can be used to determine the valence of the gaseous ions formed via ESI, see: (a) refs 53b,c, 54b, and 55. (b) Schröder, D.; Engeser, M.; Schwarz, H.; Rosenthal, E. C. E.; Döbler, J.; Sauer, J. *Inorg. Chem.* **2006**, *45*, 6235. (c) Rochut, S.; Roithová, J.; Schröder, D.; Novara, F. R.; Schwarz, H. *J. Am. Soc. Mass Spectrom.* **2008**, *19*, 121.

(59) (a) Armentrout, P. B.; Kickel, B. L. In *Organometallic Ion Chemistry*; Freiser, B. S., Ed.; Kluwer: Norwall, MA, 1996; p 1. (b) Beyer, M. K. *Mass Spectrom. Rev.* **2007**, *26*, 517.

(60) In essence, this difference can be related to the trans effect operative in $[UO_2(OH)(H_2O)_3]^+$ due to the 180° arrangement of the hydroxo and the opposite water ligand; see: Kauffmann, G. B. *J. Chem. Educ.* **1977**, *54*, 86.

(61) For a similar situation in neutral and cationic iron hydroxides and -halides, see: (a) Schröder, D.; Schwarz, H. *Int. J. Mass Spectrom.* **2003**, *227*, 121. See also: (b) Schröder, D.; Souvi, O.; Alikhani, E. *Chem. Phys. Lett.* **2009**, *470*, 162.

(62) As far as the pH of the solution is concerned, consideration of anion capture by the solvated uranyl dication UO_2^{2+} would lead to the same net balance and therefore is omitted.

Dinuclear Uranyl Cluster Cations. In addition to the mononuclear uranyl(VI) complexes mentioned above, the ESI spectra reveal the formation of several dinuclear uranyl complexes with pronounced signals at m/z 645, 708, 753, and 798, to which the compositions $[U_2O_4(OH)_3(H_2O)_3]^+$, $[U_2O_4(OH)_2(NO_3)(H_2O)_4]^+$, $[U_2O_4(OH)(NO_3)_2(H_2O)_4]^+$, and $[U_2O_4(NO_3)_3(H_2O)_4]^+$, respectively, are assigned.[36] Furthermore, weaker signals at m/z 690, 735, and 780 are observed which correspond to the less solvated ions $[U_2O_4(OH)_2(NO_3)(H_2O)_3]^+$, $[U_2O_4(OH)(NO_3)_2(H_2O)_3]^+$, and $[U_2O_4(NO_3)_3(H_2O)_3]^+$, respectively. The formation of these cluster ions can be rationalized by a combination of the mononuclear ions present in solution with neutral uranium species such as $UO_2(OH)_2$, $UO_2(OH)(NO_3)$, and $UO_2(NO_3)_2$ (Figure S1, Supporting Information), or − equivalently − solvated UO_2^{2+} recombines with anionic uranyl complexes.[26] Fully consistent with the concentration-dependent trend of the monomeric species discussed above, the signals due to $[U_2O_4(OH)_3(H_2O)_n]^+$ are quite low for all concentrations: In very diluted solutions, the hydroxo species prevail, but at the same time, clustering is disfavored by the mass-action law. At increased uranium concentration, clustering is more pronounced, but likewise the fraction of hydroxo clusters is lower (Figure 1). At larger concentrations, the most abundant dinuclear cluster is $[U_2O_4(OH)(NO_3)_2(H_2O)_3]^+$, which comprises up to 12% of the integrated abundances of uranium ions in the positive-mode ESI mass spectra.

Another notable aspect concerns the average hydration numbers of the dinuclear clusters, as these are somewhat lower for the hydroxo-rich clusters than for nitrato-rich ions, that is, $n_{av} = 3.06 \pm 0.04$ for $[U_2O_4(OH)_3(H_2O)_n]^+$, $n_{av} = 3.33 \pm 0.05$ for $[U_2O_4(OH)_2(NO_3)(H_2O)_n]^+$, $n_{av} = 3.74 \pm 0.03$ for $[U_2O_4(OH)(NO_3)_2(H_2O)_n]^+$, and $n_{av} = 3.67 \pm 0.04$ for $[U_2O_4(NO_3)_3(H_2O)_n]^+$. This behavior is attributed to the higher charge density of the uranyl unit in the contact ion pair of nitrato−uranyl $[UO_2(NO_3)]^+$ compared to the more covalent hydroxo−uranyl complex $[UO_2(OH)]^+$. In addition, the theoretical studies reveal that, for the hydroxo clusters, bridging μ-oxo ligands are also an energetically favorable alternative (see below). Further, the abundances of the different dinuclear species were found to vary with the concentration of the sprayed solution, in that the nitrato clusters are preferred at higher concentrations (Figure S2, Supporting Information). By analogy to the trend mentioned above for the mononuclear species (Figure 1), this behavior can be explained by hydrolysis occurring in solution and the associated change of pH.

The results of the CID experiments of the mass-selected cluster ions are consistent with the assumed formation of dinuclear uranium(VI) clusters with bridging anionic ligands. Figure 4 displays the CID spectra of four representative dinuclear clusters. In general, losses of water ligands from the solvation sphere of the dinuclear clusters are largely preferred. For the mixed nitrate clusters, losses of nitric acid are also observed, but their abundances are significantly lower than those of the losses of neutral water. Further, even weaker signals, which only appear at elevated collision energies, involve cluster degradation to mononuclear species via a loss of neutral uranium(VI) compounds.

The CID patterns are also quite instructive as far as cluster structures are concerned. Specifically, the pure

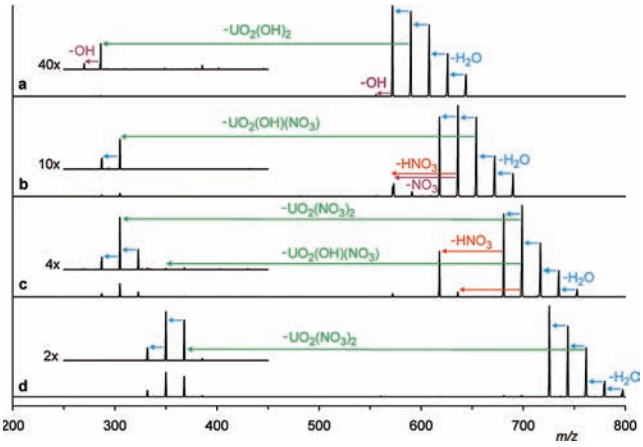

Figure 4. CID spectra of the mass-selected binuclear clusters (a) $[U_2O_4(OH)_3(H_2O)_3]^+$ (m/z 645), (b) $[U_2O_4(OH)_2(NO_3)(H_2O)_3]^+$ (m/z 690), (c) $[U_2O_4(OH)(NO_3)_2(H_2O)_4]^+$ (m/z 753), and (d) $[U_2O_4(NO_3)_3(H_2O)_4]^+$ (m/z 798) at a collision energy of E_{lab} = 20 eV. The insets show vertical enlargements of the regions m/z = 250−450 with the factors indicated.

Scheme 1. Proton Transfer from a Bridging μ-Hydroxo Ligand in a Binuclear Cluster $[U_2O_4(OH)(X)(NO_3)(H_2O)_3]^+$ (X = OH, NO_3) to Afford a μ-Oxo-Bridged Cluster from Which Neutral HNO_3 Can Be Lost

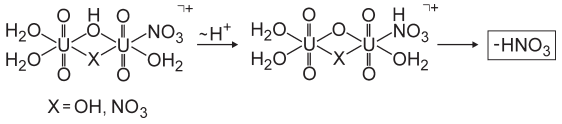

nitrato cluster $[U_2O_4(NO_3)_3(H_2O)_4]^+$ hardly undergoes a loss of HNO_3 (Figure 4d), even though the four water ligands present offer many available protons. In comparison to the notable HNO_3 losses in Figure 4b and c, this result implies that the loss of nitric acid from the cluster requires the presence of a hydroxo ligand. It appears surprising, however, that the same type of proton transfer obviously is much less favorable for the water ligands in $[U_2O_4(NO_3)_3(H_2O)_4]^+$. A possible explanation of this effect evolves from the consideration that the hydroxo unit is much more likely to act as a bridging ligand than a neutral water molecule. In a bridging position, however, deprotonation of the hydroxo unit can lead to a bridging oxo ligand, which is not accessible directly from a cluster with bridging nitrato ligands (Scheme 1). Accordingly, the CID patterns imply that hydroxo, rather than nitrato, is primarily involved as a bridging ligand and that even bridging μ-oxo ligands are accessible in the dinuclear clusters.

Another notable aspect concerns the loss of neutral uranium compounds upon cluster degradation, in that the ionic fragments show a preference for retention of hydroxo ligands (see Figure 4b and c). Hence, we conclude that either the neutral uranium nitrates or the cationic hydroxides are more stable, which is an independent experimental confirmation of the computed endothermicities of reaction 2 discussed above. Further, the amount of cluster degradation shows a remarkable increase from X and Y = OH (Figure 4a) to X and Y = NO_3 (Figure 4d), which is consistent with the hydroxo (or oxo) ligands forming strong μ-bridges, whereas the bridging mode is less favorable for nitrate.

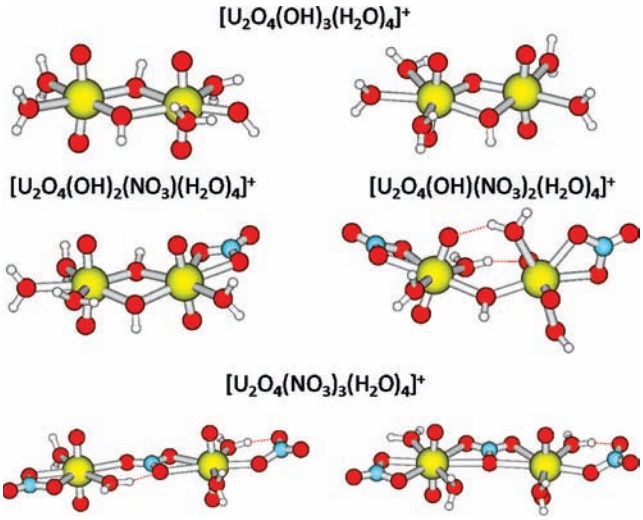

Figure 5. Representative energetically low-lying structures found in the theoretical survey of the binuclear clusters $[U_2O_4(X,Y)_3(H_2O)_4]^+$ with X, Y = OH, NO_3. Where two structures are shown, both isomers lie energetically within 0.02 eV (for details, see Supporting Information).

In the case of the gaseous dinuclear clusters with two or more hydroxo ligands, there evolves an additional structural issue with respect to the coordination sphere. Specifically, the theoretical results of Tsushima et al.[24] predict that the most stable isomer of this type of water-solvated uranyl cluster are oxo-bridged species $[U_2O_5(X)(H_2O)_{n+1}]^+$, rather than the corresponding dihydroxo isomers $[U_2O_4(OH)_2(X)(H_2O)_n]^+$ (X = OH, NO_3). In fact, the CID spectra of the dinuclear species $[U_2O_4(OH)_3(H_2O)_3]^+$ show the successive eliminations of up to four water molecules (Figure 4a), which confirms that the oxo-bridged configuration $[U_2O_5(OH)(H_2O)_n]^+$ is accessible, at least upon CID. In fact, theory even predicts favorable energetics of the oxo-bridged clusters (Figure 5).

The optimized geometries of the energetically most stable uranium(VI) ions[63] with the composition $[U_2O_4(X,Y)_3(H_2O)_4]^+$ (X, Y = OH, NO_3) are shown in Figure 5. For the formally pure hydroxo cluster $[U_2O_4(OH)_3(H_2O)_4]^+$, the most stable structures correspond to complexes with either bridging oxo- and bridging hydroxo groups or two bridging hydroxo groups between the uranium atoms and surrounding water ligands, giving rise to one hexa- and one heptacoordinated uranium center.[64] Due to the ability of nitrate to act as a bidentate ligand and the possibility of uranium adopting coordination numbers larger than 6, all nitrato clusters, however, bear a coordination number of 7. In the mixed clusters $[U_2O_4(OH)_2(NO_3)(H_2O)_4]^+$ and $[U_2O_4(OH)(NO_3)_2(H_2O)_4]^+$, there is great preference for the hydroxy groups acting as bridging ligands, whereas in $[U_2O_4(NO_3)_3(H_2O)_4]^+$, a μ-nitrato bridge with an additional hydrogen bond is realized in the most stable structure found. However, a $[U_2O_4(NO_3)_3(H_2O)_4]^+$ structure with a bridging nitrato group without any hydrogen bond connected to it lies less than 0.02 eV higher in energy. These computational results are in pleasing agreement with the qualitative structural conclusions derived from the CID experiments discussed above.

Higher Uranyl Cluster Cations. Though much less abundant, larger oligomeric uranyl species are also observed, such as tri-, tetra-, and pentanuclear clusters $[(U_mO_{2m}(X,Y)_{2m-1}(H_2O)_n]^+$ (X, Y = OH, NO_3; m = 3−5, n = 1−3). The formation of these adducts is strongly dependent on the concentration of the sprayed solution. Specifically, significant amounts of the dinuclear clusters are already observed in the ESI spectrum of the sprayed solution with the lowest concentration (1×10^{-8} mol L^{-1}), whereas the trinuclear species start to be formed at a concentration of ca. 5×10^{-7} mol L^{-1}. A further increase in the concentration causes the formation of tetranuclear (at about 10^{-6} mol L^{-1}) and pentanuclear clusters (at about 7×10^{-5} mol L^{-1}). These results clearly indicate that the formation of uranyl adducts is favored when the concentration of the sprayed solution increases, thereby indicating that the clustering is a direct response to the solution properties. While we cannot strictly exclude the possibility that the association only occurs in the ESI process itself, there exists ample evidence for the formation of uranium clusters in the solution phase.[24,29] The trend for the gaseous clusters to increase with the concentration of the sprayed solution follows a similar tendency occurring in solution and can thus be rationalized qualitatively in terms of the mass-action law. In other words, the degree of long-range electrostatic interactions and thus ion aggregation (ion association) in solution tends to be amplified with increasing concentration,[65] which is reflected by the larger amount of the gaseous cluster ions at higher concentrations of the sprayed solutions.

Fragmentation pathways analogous to the dinuclear species were observed upon CID of the larger clusters, namely, losses of the coordinated water molecules at low collision energies and the expulsion of either $UO_2(NO_3)_2$, $UO_2(OH)(NO_3)$, or $UO_2(OH)_2$ units at elevated collision energies, resulting in cluster degradation. By reference to the concept of microscopic reversibility, these fragmentation pathways indicate that the associated neutral uranyl species $UO_2(NO_3)_2$, $UO_2(OH)NO_3$, and $UO_2(OH)_2$ also play a role in the formation of the clusters. The dinuclear cations observed, for example, can be formed by the addition of $UO_2(NO_3)_2$, $UO_2(OH)(NO_3)$, and $UO_2(OH)_2$ to either $[UO_2(OH)(H_2O)_n]^+$ or $[UO_2(NO_3)(H_2O)_n]^+$. Accordingly, the trinuclear, tetranuclear, and pentanuclear complexes are most probably generated through the addition of mononuclear, neutral uranyl species to dinuclear, trinuclear, and tetranuclear complexes, respectively (see Figure S2, Supporting Information). Such a mechanism of adduct formation can easily explain the preferential elimination of the associated uranyl species upon CID and is consistent with the trend for clustering upon rising concentrations of sprayed solution in terms of

(63) For reduced uranium species bearing peroxidic ligands, see also: Bryantsev, V. S.; de Jong, W. A.; Cossel, K. C.; Diallo, M. S.; Goddard, W. A., III; Groenewold, G. S.; Chien, W.; Van Stipdonk, M. J. *J. Phys. Chem. A* **2008**, *112*. 5777.

(64) The genuine trishydroxo cluster $[U_2O_4(OH)_3(H_2O)_4]^+$ with two bridging and one terminal hydroxo ligand is 0.05 eV higher in energy than the μ-oxo cluster shown in Figure 5.

(65) Powell, K. J.; Brown, P. L.; Byrne, R. H.; Gajda, T.; Hefter, G.; Sjøberg, S.; Wanner, H. *Pure Appl. Chem.* **2007**, *79*, 895.

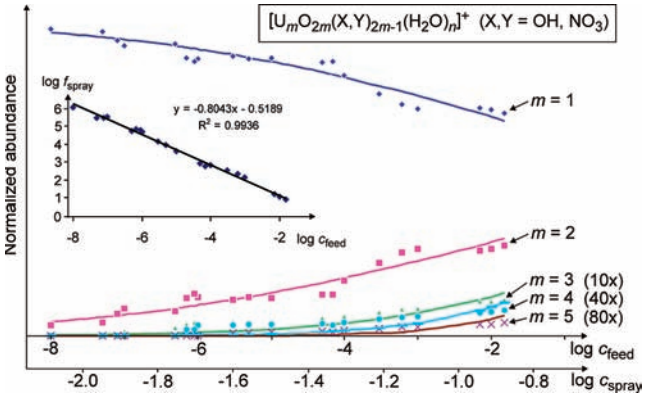

Figure 6. Normalized ion abundances of the mono- and oligonuclear species $[U_mO_{2m}(X,Y)_{2m-1}(H_2O)_n]^+$ (X, Y = OH, NO_3) in the ESI mass spectra of $UO_2(NO_3)_2$ in water as a function of the concentration of the feed solutions (c_{feed}) of the ESI source and the derived concentration in the electrospray process (c_{spray}).

an amplification of the degree of ion association and, thus, increased amounts of neutral ion pairs in solution.[26]

Concentration Dependence of the Cluster Cations. Figure 6 summarizes the variation of the cluster-ion sizes with the concentration of the feed solution (c_{feed}) admitted to the ESI source. A close qualitative correlation between the ESI mass spectra and the solution properties is obvious. The key question is, however, whether there also exists some quantitative correlation. Consideration of the basics of the ESI process implies that the concentration of the solution in the spray process (c_{spray}) is very likely to differ from c_{feed}. In brief, ESI involves pumping a feed solution through a small capillary which is charged to a high voltage. The voltage and additional flow of nitrogen gas lead to the formation of droplets in the form of a spray, and these droplets shrink in the subsequent regions of the ESI source (often with assistance from a section at an elevated temperature). At a certain critical droplet size or jet diameter, gaseous ions are formed from the solution, which are then transferred to the mass spectrometer via a differential pumping system. As a considerable share of the solvent evaporates before the ions are formed, the nonvolatile components (i.e., the uranium salt) are thus more concentrated in the spray process than in the feed solution.[66,67] For slow equilibria (e.g., host−guest complexes), these changes in concentration do not play a role because the droplet evaporation in ESI is too fast, whereas for fast processes (e.g., ion pairing of inorganic salts in aqueous solution), these changes in the ESI process may be decisive.[37] For the present case of uranyl nitrate in water, it is obvious that the latter situation applies, because at concentrations in the range of 10^{-8} mol L^{-1} neither the nitrato complexes $[UO_2(NO_3)(H_2O)_n]^+$ nor any clusters should be observed due to the extreme dilution.[24,29,39] In order to account for this change in concentration, we define the purely phenomenological relation $c_{spray} = f_{spray} \times c_{feed}$, where f_{spray} is the enrichment factor ($f_{spray} > 1$). Further, consideration of the extremes of the concentrations investigated here implies that f_{spray} is unlikely to be constant but is, rather, expected to depend on c_{feed}. Hence, even if evaporated to dryness, the most concentrated solution used ($c_{feed} = 1.5 \times 10^{-2}$ mol L^{-1}) can maximally exhibit $f_{spray,max} \approx 370$,[68,69] whereas much larger values are conceivable for lower-concentration solutions, for example, $f_{spray,max} \approx 5 \times 10^8$ for the most dilute solution investigated ($c_{feed} = 10^{-8}$ mol L^{-1}). In order to further substantiate the latter, seemingly very large factor for the solution with the lowest concentration, it is to be considered that the ESI mass spectra only sample those droplets which contain a metal ion, whereas all droplets consisting of pure water escape detection. In part, this is reflected by the total ion current of the electrospray, but ESI is charge-limited in that the spray current is proportional to concentration only in a narrower range than the various concentrations which still can be measured using ESI.[31,70] While the conclusion that $f_{spray} > 1$ is thus obvious, the absolute value of f_{spray} is unknown, and hence a conversion of c_{feed} into c_{spray} cannot be made. A further analysis of the correlation between the cluster sizes and c_{feed} clearly evident in Figure 6 is thus impossible without additional assumptions. In this context, we would like to point out explicitly two essentials. On the one hand, the relation $c_{spray} = f_{spray} \times c_{feed}$ inherently applies equilibrium considerations to a highly dynamical process such as electrospray ionization and is thus questionable from first principle considerations. While more advanced treatments have been realized,[38] these require extensive modeling efforts and additional input from theory. On the other hand, we deliberately aim toward a practical—and here this means an empirical—relationship between the macroscopic concentration and the microscopic ion patterns observed in the ESI mass spectra. Only if such a reasonably simple approach would be applicable, could it promote further usage of ESI in element speciation.[26,27a] Instead, a more comprehensive treatment, which takes nonequilibrium effects into account,[38] would most likely consume more input in terms of basic research than provide output for applied sciences.

To a first approximation, a value of $f_{spray}(1.5 \times 10^{-2}$ mol $L^{-1}) \approx 8$ can be derived from conductivity data, which suggests an association constant of about $K_a = (6.6 \pm 0.4)$ for aqueous uranyl nitrate (see the Supporting Information).[71,72] We would like to stress, however, that at this stage our aim is mostly a methodological proof of concept of the approach rather than a precise determination of the absolute association constants of uranyl nitrate in aqueous solution.[40] None of the qualitative

(66) (a) Wang, H. J.; Agnes, G. R. *Anal. Chem.* **1999**, *71*, 3785. (a) Wang, H. J.; Agnes, G. R. *Anal. Chem.* **1999**, *71*, 4166. (c) Bakhoum, S. F. W.; Agnes, G. R. *Anal. Chem.* **2005**, *77*, 3189.

(67) Wang, G. D.; Cole, R. B. *Anal. Chim. Acta* **2000**, *406*, 53.

(68) This maximal value is based on the density of solid uranyl nitrate hexahydrate with the assumption that the solvent is evaporated completely. For the solubility of this compound in hot water, 1.2 mol L^{-1}, $f_{spray,max}$ would be about 100.

(69) For modeling properties of concentrated solutions of uranyl nitrate, see: Ruas, A.; Bernard, O.; Caniffi, B.; Simonin, J.-P.; Turq, P.; Blum, L.; Moisy, P. *J. Phys. Chem. B* **2006**, *110*, 3435.

(70) (a) Zook, D. R.; Bruins, A. P. *Int. J. Mass Spectrom. Ion Processes* **1997**, *162*, 129. (b) Gatlin, C. L.; Tureček, F. *J. Mass Spectrom.* **2000**, *35*, 172.

(71) Earlier conductivity data with a much more limited range of $UO_2(NO_3)_2$ concentrations yielded $K_a = 3$, which implies $f_{spray}(1.5 \times 10^{-2}$ mol $L^{-1}) \approx 20$. For the original data, see ref 46.

(72) A value of $f_{spray}(1.5 \times 10^{-2}$ mol $L^{-1}) \approx 2$ can be derived from the difference of the R_{free} value of 0.89 determined from ESI data and the conductivity ratio of $\Lambda_{0.001}/\Lambda_0 = 0.917$ found in the same work; for further details and definitions, see: Megyes, T.; Radnai, T.; Wakisaka, A. *J. Phys. Chem. A* **2002**, *106*, 8059.

conclusions below, for example, is changed when the initial guess of $f_{spray}(1.5 \times 10^{-2}$ mol $L^{-1}) \approx 8$ is changed to either 2 or 20.[71,72] The strategy to determine c_{spray} from the experimental patterns in Figure 6 is as follows. At first, we integrate the intensities of all $[U_mO_{2m}(X,Y)_{2m-1}(H_2O)_n]^+$ species for a given value of m to arrive at the nominal intensities of the various cluster ions with $m = 1-5$, irrespective of the nature of the counterions X and Y as well as the number of water ligands n. Second, we assume that the association of all of these cations with the neutral uranium species present in solution can be described by a single set of equilibrium constants, $K(m) = k_f(m) \times c_{spray}/k_b(m)$; for $m = 1$, $k_f(1)$ thus stands for the rate constant of association of the monomeric cations with neutral uranium species $UO_2(X,Y)_2$ to form dinuclear clusters, and $k_b(1)$ represents the corresponding reverse reaction. With these assumptions and the above estimate of $f_{spray}(1.5 \times 10^{-2}$ mol $L^{-1}) \approx 8$ as an additional input for $K(1)$, the data can be subjected to a kinetic modeling which comprises an explicit treatment of the time evolution of the $[U_mO_{2m}(X,Y)_{2m-1}(H_2O)_n]^+$ population until a steady state is reached.[73] In this procedure, first the $K(m)$ values with $m > 1$ are fitted to the most concentrated solution for which $f_{spray} = 8$ is assumed, and then the c_{spray} of the other solutions is adjusted to fit the measured intensity patterns for $m = 1-5$ without further adjustment of the $K(m)$ values. In the next step, the resulting values of c_{spray} are converted into f_{spray}, which is plotted over c_{feed}. The resulting linear correlation between $\log(f_{spray})$ and $\log(c_{feed})$, shown in the inset of Figure 6, is then used to replace the fitted values of c_{spray} with the term $f_{spray} \times c_{feed}$. The result of this modeling is included in Figure 6 along with the experimental data points (dots). Thus, the solid lines show the concentration patterns of the various cluster sizes derived with this approach, and the inset shows a double logarithmic plot of f_{spray} over c_{feed}.

While the quality of the fits is moderate only and the kinetic modeling is based on several assumptions, the results have some useful implications with regard to possible correlations between ESI mass spectra and the speciation of uranyl nitrate in aqueous solution. At first, the linear correlation of $\log f_{spray}$ and $\log c_{feed}$ lends support to the anticipated relationship between these parameters outlined above. Second, the enrichment factor increases from $f_{spray} \approx 12$ for 10^{-2} mol L^{-1} up to $f_{spray} \approx 6 \times 10^5$ for the most dilute solution (10^{-8} mol L^{-1}), where the trend is expected, while the absolute values of f_{spray} for low concentrations might appear surprisingly large. However, the large values of f_{spray} are a direct consequence of the high selectivity of ESI in which ionic compounds, here, the uranium species, are sampled preferentially. Further, the values of $K(m)$ resulting from the modeling drop from the assumed value of 6.6 for the formation of the dinuclear cluster to ca. 0.65 for the trinuclear species and then increase to values of about 2.7 and 5 for the tetra- and pentanuclear clusters, respectively, indicating that the clustering of the uranium species does not follow a merely statistical trend but instead size-dependent selectivities are operative, as is also indicated by condensed-phase data.[24,29,39] These size dependencies are also reflected directly in the experimental data, in that the larger clusters ($m = 4$, 5) bear significant abundances already at low concentrations (Figure 6). We note in passing that, after rescaling the concentrations c_{feed} in Figure 1 to c_{spray}, the ratio of the uranium-hydroxo versus -nitrato complexes is in reasonable agreement with the data known about the speciation of uranium nitrate in aqueous solution (Figure S3, Supporting Information), as indicated by the horizontal bars on top of Figure 1.[40]

Several limitations of the modeling are obvious, however, and particularly the abundances of the tetranuclear species are significantly underestimated at low concentrations. These deviations might be coped with by explicit consideration of the counterions in the various clusters, unlike the mere cluster size considered in this simple model, and by the inclusion of the larger clusters in the association, as the present model only includes the association of $[U_mO_{2m}(X,Y)_{2m-1}(H_2O)_n]^+$ (X,Y = OH, NO_3) with monomeric $UO_2(X,Y)_2$. Notwithstanding these limitations, the results are regarded as a significant step toward a direct correlation between ESI data and the speciation behavior of metal salts in aqueous solution. Moreover, the values of f_{spray} are obviously characteristic for each solvent as well as the ionization conditions, but it appears plausible that they are independent from the metal salt as long as the solvent is present in large excess. However, while the correlations are obvious, the precise quantitative interpretation yet relies upon several assumptions and the dependencies of the larger clusters are not reproduced perfectly. Furthermore, the ratios of the different cluster sizes somewhat depend on the experimental conditions. Thus, variation of the conditions in electrospray ionization reveals that the precise ratios between monomeric and oligomeric ions are influenced by several parameters, such as the flow rate of the aqueous solution of uranyl nitrate and that of the nitrogen bath gas and the temperature of the transfer capillary. An increased flow rate of the feed solution, for example, increases the amount of mononuclear species in the resulting mass spectra, pointing to a decrease in f_{spray}, which appears physically reasonable. These observations imply, however, that an absolute quantification of ion speciation using ESI requires anchoring to at least one independent experiment conducted in solution.[28,74,75] While this certainly is a significant drawback of ESI, the conceptual advantage is the ability to directly and simultaneously monitor the molecular species involved in ion speciation, rather than determining sum parameters, as is usually the case for condensed-phase studies.[26,76]

(73) (a) Schröder, D.; Schwarz, H. *Angew. Chem., Int. Ed. Engl.* **1990**, *29*, 1431. (b) Schröder, D.; Brown, R.; Schwerdtfeger, P.; Schwarz, H. *Int. J. Mass Spectrom.* **2000**, *203*, 155. (c) Butschke, B.; Schlangen, M.; Schwarz, H.; Schröder, D. *Z. Naturforsch., B: Chem. Sci.* **2007**, *62b*, 309.

(74) (a) Di Marco, V. B.; Bombi, G. G.; Tubaro, M.; Traldi, P. *Rapid Commun. Mass Spectrom.* **2003**, *17*, 2039. (b) Di Marco, V. B.; Bombi, G. G.; Ranaldo, M.; Traldi, P. *Rapid Commun. Mass Spectrom.* **2007**, *21*, 3825. (c) Di Marco, V. B.; Bombi, G. G. *J. Mass Spectrom.* **2009**, *44*, 120.

(75) (a) Hartman, J. R.; Vachet, R. W.; Pearson, W.; Wheat, R. J.; Callahan, J. H. *Inorg. Chim. Acta* **2003**, *343*, 119. (b) Hartman, J. R.; Combariza, M. Y.; Vachet, R. W. *Inorg. Chim. Acta* **2004**, *357*, 51. (c) Hartman, J. A. R.; Kammier, A. L.; Spracklin, R. J.; Pearson, W. H.; Combariza, M. Y.; Vachet, R. W. *Inorg. Chim. Acta* **2004**, *357*, 1141.

(76) (a) Hao, C.; March, R. E.; Croley, T. R.; Smith, J. C.; Rafferty, S. P. *J. Mass Spectrom.* **2001**, *36*, 79. (b) Hao, C.; March, R. E. *J. Mass Spectrom.* **2001**, *36*, 509.

Conclusions

The speciation of uranyl nitrate in aqueous solution is studied by means of ESI mass spectrometry. A detailed analysis of the concentration-dependent behavior of the observed gaseous $[U_mO_{2m}(X,Y)_{2m-1}(H_2O)_n]^+$ cations (X, Y = OH, NO_3; $m = 1-5$) reveals several correlations with the situation that exists in solution. Thus, the predominance of either nitrato- or hydroxo-uranyl species is controlled by the concentration and hence the extent of the hydrolysis in aqueous solution. Further, the tendency for formation of gaseous clusters, either preformed in solution or generated during the spray process, shows a clear correlation with the concentration of the feed solution. Thus, the amplification of ion association with rising concentration in solution leads to an analogous enhancement of the cluster-ion signals in the gas-phase measurements. The data are used to propose an approximate relationship between the gas-phase data and the concentrations in solution, which suggests that the effective metal concentrations can increase by factors close to 10^6 in the course of the electrospray process. The details of the correlations between the ESI data and the behavior in solution still need to be elucidated further, and the uranium system considered here is obviously not ideal due to its complexity, although the latter also offers some advantages due to the existence of more than a single correlation between gas-phase and condensed-phase distributions. Nevertheless, we believe that the present work strongly suggests mass spectrometric methods as complementary tools to achieve insight into the speciation of metals on a molecular level.

Acknowledgment. This work was supported by the Academy of Sciences of the Czech Republic (Z40550506), the Grant Agency of the Czech Republic (203/08/1487), and the Ministry of Education of the Czech Republic (MSM0021620857). PS acknowledges postdoctoral grant 203/07/P449 and computational support of the Center for complex molecular systems (grant LC512 by the Ministry of Education of the Czech Republic).

Supporting Information Available: Tables reporting the chemical compositions, the mass-to-charge ratios, and the relative intensities of gaseous ions formed upon ESI of selected aqueous solutions of uranyl nitrate, conductivity data, supplementary schemes, and computed structures and total energies are available free of charge via the Internet at http://pubs.acs.org.